Inorganic Chemistry
Article

Inorg. Chem. **2010**, *49*, 11627–11636 **11627**
DOI: 10.1021/ic1020737

Syntheses and Crystal Structures of a Series of Alkaline Earth Vanadium Selenites and Tellurites

Su-Yun Zhang,[†,‡] Chun-Li Hu,[†] Chuan-Fu Sun,[†] and Jiang-Gao Mao*[,†]

[†]*State Key Laboratory of Structural Chemistry, Fujian Institute of Research on the Structure of Matter, Chinese Academy of Sciences, Fuzhou 350002, P.R. China, and* [‡]*Graduate School of the Chinese Academy of Sciences, Beijing 100039, P.R. China*

Received October 13, 2010

Six new novel alkaline-earth metal vanadium(V) or vanadium(IV) selenites and tellurites, namely, $Sr_2(VO)_3(SeO_3)_5$, $Sr(V_2O_5)(TeO_3)$, $Sr_2(V_2O_5)_2(TeO_3)_2(H_2O)$, $Ba_3(VO_2)_2(SeO_3)_4$, $Ba_2(VO_3)Te_4O_9(OH)$, and $Ba_2V_2O_5(Te_2O_6)$, have been prepared and structurally characterized by single crystal X-ray diffraction analyses. These compounds exhibit six different anionic structures ranging from zero-dimensional (0D) cluster to three-dimensional (3D) network. $Sr_2(VO)_3(SeO_3)_5$ features a 3D anionic framework composed of VO_6 octahedra that are bridged by SeO_3 polyhedra. The oxidation state of the vanadium cation is +4 because of the partial reduction of V_2O_5 by SeO_2 at high temperature. $Ba_3(VO_2)_2(SeO_3)_4$ features a 0D $[(VO_2)(SeO_3)_2]^{3-}$ anion. $Sr(V_2O_5)(TeO_3)$ displays a unique 1D vanadium(V) tellurite chain composed of V_2O_8 and V_2O_7 units connected by tellurite groups, forming 4- and 10-MRs, whereas $Sr_2(V_2O_5)_2(TeO_3)_2(H_2O)$ exhibits a 2D layer consisting of $[V_4O_{14}]$ tetramers interconnected by bridging TeO_3^{2-} anions with the Sr^{2+} and water molecules located at the interlayer space. $Ba_2(VO_3)Te_4O_9(OH)$ exhibits a one-dimensional (1D) vanadium tellurite chain composed of a novel 1D $[Te_4O_9(OH)]^{3-}$ chain further decorated by VO_4 tetrahedra. $Ba_2V_2O_5(Te_2O_6)$ also features a 1D vanadium(V) tellurites chain in which neighboring VO_4 tetrahedra are bridged by $[Te_2O_6]^{4-}$ dimers. The existence of V^{4+} ions in $Sr_2(VO)_3(SeO_3)_5$ is also confirmed by magnetic measurements. The results of optical diffuse-reflectance spectrum measurements and electronic structure calculations based on density functional theory (DFT) methods indicate that all six compounds are wide-band gap semiconductors.

Introduction

Metal selenites and tellurites can form a diversity of unusual structures as a result of the presence of the stereochemically active lone-pair electrons which could serve as a structure-directing agent.[1] The asymmetric coordination polyhedron of the Se(IV) or Te(IV) atom caused by so-called second-order Jahn−Teller (SOJT) distortion associated with s-p mixing may also result in non-centrosymmetric (NCS) structures with consequent interesting physical properties, such as non-linear optical second harmonic generation (SHG).[2] Transition metal ions with d^0 electronic configurations such as Ti^{4+}, V^{5+}, and Mo^{6+}, which are also susceptible to SOJT distortion, have been introduced to metal selenites and tellurites systems to reinforce the polarizations of these structures by the additive polarization of both types of asymmetric polyhedra.[3] So far, many research works have been done on combining the above two types of cations in the same compound, and various types of metal ions have been used as the counter-cations to balance the excess negative charges of the anionic architectures, such as the alkali or NH_4^+ ions and alkaline-earth ions,[4] transition-metal ions excluding those with d^0 electronic configurations,[5] post-transition metal

*To whom correspondence should be addressed. E-mail: mjg@fjirsm.ac.cn.

(1) Wickleder, M. S. *Chem. Rev.* **2002**, *102*, 2011, and references therein.

(2) (a) Kim, S.-H.; Yeon, J.; Halasyamani, P. S. *Chem. Mater.* **2009**, *21*, 5335. (b) Ok, K.-M.; Bhuvanesh, N. S. P.; Halasyamani, P. S. *Inorg. Chem.* **2001**, *40*, 1978. (c) Kong, F.; Huang, S. P.; Sun, Z. M.; Mao, J. G.; Cheng, W. D. *J. Am. Chem. Soc.* **2006**, *128*, 7750. (d) Porter, Y.; Bhuvanesh, N. S. P.; Halasyamani, P. S. *Inorg. Chem.* **2001**, *40*, 1172. (e) Kim, M. K.; Kim, S.-H.; Chang, H.-Y.; Halasyamani, P. S.; Ok, K. M. *Inorg. Chem.* **2010**, *49*, 7028.

(3) (a) Ra, H.-S.; Ok, K.-M.; Halasyamani, P. S. *J. Am. Chem. Soc.* **2003**, *125*, 7764. (b) Ok, K.-M.; Halasyamani, P. S. *Inorg. Chem.* **2004**, *43*, 4248. (c) Chang, H.-Y.; Kim, S. W.; Halasyamani, P. S. *Chem. Mater.* **2010**, *22*, 3241. (d) Chang, H. Y.; Kim, S.-H.; Ok, K.-M.; Halasyamani, P. S. *Chem. Mater.* **2009**, *21*, 1654. (e) Jiang, H. L.; Huang, S. P.; Fan, Y.; Mao, J. G. *Chem.—Eur. J.* **2008**, *14*, 1972. (f) Ok, K. M.; Halasyamani, P. S. *Chem. Soc. Rev.* **2006**, *35*, 710.

(4) (a) Porter, Y.; Halasyamani, P. S. *J. Solid State Chem.* **2003**, *174*, 441. (b) Harrison, W. T. A.; Dussack, L. L.; Jacobson, A. J. *Inorg. Chem.* **1994**, *33*, 6043. (c) Johnston, M. G.; Harrison, W. T. A. *Acta Crystallogr., Sect. C* **2007**, *63*, i57. (d) Hou, J. Y.; Huang, C. C.; Zhang, H. H.; Tu, C. Y.; Sun, R. Q.; Yang, Q. Y. *J. Mol. Struct.* **2006**, *785*, 37. (e) Harrison, W. T. A.; Dussack, L. L.; Jacobson, A. J. *J. Solid State Chem.* **1996**, *125*, 234. (f) Kwon, Y.-U.; Lee, K.-S.; Kim, Y. H. *Inorg. Chem.* **1996**, *35*, 1161.

(5) (a) Zhang, S. Y.; Jiang, H. L.; Sun, C. F.; Mao, J. G. *Inorg. Chem.* **2009**, *48*, 11809. (b) Jiang, H. L.; Xie, Z.; Mao, J. G. *Inorg. Chem.* **2007**, *46*, 6495. (c) Ling, J.; Albrecht-Schmitt, T. E. *J. Solid State Chem.* **2007**, *180*, 1601. (d) Zhou, Y.; Hu, C. L.; Hu, T.; Kong, F.; Mao, J. G. *Dalton Trans.* **2009**, 5747. (e) Pitzschke, D.; Jansen, M. *Z. Anorg. Allg. Chem.* **2007**, *633*, 1563. (f) Zhang, D.; Johnsson, M. *Acta Crystallogr., Sect. C* **2009**, *65*, i9.

Published on Web 11/23/2010

main-group IIIA cations (such as Ga^{3+} /In^{3+})[6] as well as the lanthanide(III) ions.[7] A number of actinide selenites and tellurites (mostly U(VI), Np(IV), and Th(IV)) have been reported by Albrecht-Schmitt et al. and Krivovichev et al.[8] Furthermore, several phases of Tl^{+}, Pb^{2+}, and Bi^{3+} cations with lone pair electrons have been also reported.[2a,b,3b,3c,9]

Most studies on alkaline-earth selenites and tellurites decorated by d^0 transition metal ions are dominated by the $Ba^{II}-Mo^{VI}/W^{VI}-Se^{IV}/Te^{IV}-O$ combinations, and only three compounds containing V^{4+} or V^{5+} cations were reported, namely, one-dimensional (1D) BaV_2TeO_8, two-dimensional (2D) $Ba_{2.5}(VO_2)_3(SeO_3)_4 \cdot H_2O$, and three-dimensional (3D) $Ba(VO_2)(SeO_3)_2(HSeO_3)$.[10] BaV_2TeO_8 features a 1D anionic ribbon composed of $[VTeO_6]_n$ chains connected by $[V_2O_8]$ moieties via edge-sharing. $Ba_{2.5}(VO_2)_3(SeO_3)_4 \cdot H_2O$ exhibits a 2D layered structure consisting of VO_5 square pyramids linked by SeO_3 polyhedra. $Ba(VO_2)(SeO_3)_2(HSeO_3)$ features a 3D anionic framework composed of VO_6 octahedra, SeO_3 and $HSeO_3$ polyhedra.

It is noted that vanadium and tellurium can adopt various coordination geometries so as to form a rich structural chemistry for vanadium tellurites. Vanadium usually exhibits three types of coordination modes, VO_4 tetrahedron, VO_5 square pyramid or trigonal bipyramid, and VO_6 octahedron. Furthermore, vanadium has readily accessible oxidation states from +2 to +5; tetra or pentavalent vanadium is observed in the majority of compounds synthesized by hydrothermal reactions.[3d,e,5e,5f,9−11] On the other hand, tellurium can be three-, four-, or five- coordinated, and these $Te^{IV}O_x$ ($x = 3-5$)[12] polyhedra may polymerize into various isolated clusters or extended structures. But for metal selenites, only SeO_3^{2-} and $Se_2O_5^{2-}$ have been reported, resulting in totally different structures from the corresponding tellurites. Furthermore, the structures of vanadium seleites or tellurites may also be affected by the size of the charge-balance alkaline earth metal ions. Hence, we deem it is necessary to explore the compounds in the alkaline earth-$V^{V}/V^{IV}-Se^{IV}/Te^{IV}-O$ systems systematically. Our research effort in this aspect afforded six new compounds with different structures, namely, $Sr_2(VO)_3(SeO_3)_5$, $Sr(V_2O_5)(TeO_3)$, $Sr_2(V_2O_5)_2(TeO_3)_2(H_2O)$, $Ba_3(VO_2)_2(SeO_3)_4$, $Ba_2(VO_3)Te_4O_9(OH)$, and $Ba_2V_2O_5(Te_2O_6)$. Herein, we report their syntheses and crystal and band structures as well as their optical properties.

Experimental Section

Materials and Methods. All of the chemicals were analytically pure from commercial sources and used without further purification. $SrCO_3$, $BaCO_3$, $Ba(OH)_2 \cdot 8H_2O$, $NaVO_3 \cdot 2H_2O$, and V_2O_5 were purchased from the Shanghai Reagent Factory (AR, 90.0 +%); SeO_2 (99+ %), and TeO_2 (99 +%) were purchased from ACROS ORGANICS. IR spectra were recorded on a Magna 750 FT-IR spectrometer as KBr pellets in the range of 4000−400 cm^{-1}. Microprobe elemental analyses were performed on a field emission scanning electron microscope (FESEM, JSM6700F) equipped with an energy dispersive X-ray spectroscope (EDS, Oxford INCA). The X-ray powder diffraction data were collected on a XPERT-MPD θ-2θ diffractometer or MiniFlex diffractometer using graphite-monochromated Cu Kα radiation in the 2θ range of 5−85°. Optical diffuse reflectance spectra were measured at room temperature with a PE Lambda 900 UV−visible spectrophotometer. $BaSO_4$ plate was used as a standard (100% reflectance). The absorption spectrum was calculated from reflectance spectra using the Kubelka−Munk function: $\alpha/S = (1 - R)^2/2R$,[13] where α is the absorption coefficient, S is the scattering coefficient which is practically wavelength independent when the particle size is larger than 5 μm, and R is the reflectance. Thermogravimetric analyses (TGA) were carried out with a NETZSCH STA 449C unit at a heating rate of 15 °C/min from room temperature to 1200 °C under a N_2 atmosphere. Magnetic susceptibility measurements on polycrystalline samples were performed with a PPMS-9T magnetometer at a field of 1000 Oe in the temperature range 2−300 K. The raw data were corrected for the susceptibility of the container and the diamagnetic contributions of the samples using Pascal's constants.[14]

Preparation of $Sr_2(VO)_3(SeO_3)_5$. A mixture of $SrCO_3$ (0.0296 g, 0.2 mmol), V_2O_5 (0.0364 g, 0.2 mmol), SeO_2 (0.0888 g, 0.8 mmol), and H_2O (4 mL) was sealed in an autoclave equipped with a Teflon linear (23 mL) and heated at 230 °C for 4 days, followed by slow cooling to room temperature at a rate of 6 °C/h. Green needle-shaped crystals of $Sr_2(VO)_3(SeO_3)_5$ were obtained as single phase in a yield of about 49% based on Sr. The final pH value of the reaction media is close to 2.0. The reagent of V_2O_5 has been reduced to +4, probably by oxidation of SeO_2, and the reduction reaction has been observed in the literature about vanadium(IV) selenites.[15] When VO_2 was used instead of V_2O_5, $Sr_2(VO)_3(SeO_3)_5$ could also be obtained by the hydrothermal reactions at 180 °C. The purity of the single phase was confirmed by X-ray diffraction (XRD) studies (Supporting Information, Figure S1). The energy-dispersive spectrometry (EDS) elemental analyses gave an average molar ratio of Sr/V/Se of 1.0:1.33:2.59, which is in good agreement with the one determined from single-crystal X-ray structural studies.

Preparation of $Sr(V_2O_5)(TeO_3)$ and $Sr_2(V_2O_5)_2(TeO_3)_2(H_2O)$. Single crystals of $Sr(V_2O_5)(TeO_3)$ and $Sr_2(V_2O_5)_2(TeO_3)_2(H_2O)$ (both prism in shape and orange in color) were initially obtained by hydrothermal reactions of a mixture containing $SrCO_3$, V_2O_5, TeO_2 in a molar ratio of 1:1:1 in H_2O (4 mL) sealed in an autoclave equipped with a Teflon linear

(6) (a) Kong, F.; Hu, C. L.; Hu, T.; Zhou, Y.; Mao, J. G. *Dalton Trans.* **2009**, 4962. (b) Ok, K. M.; Halasyamani, P. S. *Chem. Mater.* **2002**, *14*, 2360. (c) Ok, K. M.; Halasyamani, P. S. *Chem. Mater.* **2001**, *13*, 4278.

(7) (a) Shen, Y. L.; Jiang, H. L.; Xu, J.; Mao, J. G.; Cheah, K. W. *Inorg. Chem.* **2005**, *44*, 9314. (b) Jiang, H. L.; Ma, E.; Mao, J. G. *Inorg. Chem.* **2007**, *46*, 7012.

(8) (a) Krivovichev, S. V.; Kahlenberg, V.; Kaindl, R.; Mersdorf, E.; Tananaev, I. G.; Myasoedov, B. F. *Angew. Chem., Int. Ed.* **2005**, *44*, 1134. (b) Almond, P. M.; Sykora, R. E.; Skanthakumar, S.; Soderholm, L.; Albrecht-Schmitt, T. E. *Inorg. Chem.* **2004**, *43*, 958. (c) Sullens, T. A.; Almond, P. M.; Byrd, J. A.; Beitz, J. V.; Bray, T. H.; Albrecht-Schmitt, T. E. *J. Solid State Chem.* **2006**, *179*, 1192. (d) Woodward, J. D.; Almond, P. M.; Albrecht-Schmitt, T. E. *J. Solid State Chem.* **2004**, *177*, 3971. (e) Woodward, J. D.; Albrecht-Schmitt, T. E. *J. Solid State Chem.* **2005**, *178*, 2922. (f) Sullens, T. A.; Albrecht-Schmitt, T. E. *Inorg. Chem.* **2005**, *44*, 2282.

(9) Li, P. X.; Kong, F.; Hu, C. L.; Zhao, N.; Mao, J. G. *Inorg. Chem.* **2010**, *49*, 5943.

(10) (a) Hou, J. Y.; Huang, C. C.; Zhang, H. H.; Yang, Q. Y.; Chen, Y.-P.; Xu, J.-F. *Acta Crystallogr., Sect. C* **2005**, *61*, i59. (b) Sivakumar, T.; Ok, K. M.; Halasyamani, P. S. *Inorg. Chem.* **2006**, *45*, 3602. (c) Harrison, W. T. A.; Vaughey, J. T.; Goshorn, J. W. *J. Solid State Chem.* **1995**, *116*, 77.

(11) (a) Kim, Y. H.; Lee, K.-S.; Kwon, Y.-U. *Inorg. Chem.* **1996**, *35*, 7394. (b) Rozier, P.; Vendier, L.; Galy, J. *Acta Crystallogr., Sect. C* **2002**, *58*, i111. (c) Xiao, D. R.; Wang, S. T.; Wang, E. B.; Hou, Y.; Li, Y. G.; Hu, C. W.; Xu, L. *J. Solid State Chem.* **2003**, *176*, 159. (d) Halasyamani, P. S.; O'Hare, D. *Inorg. Chem.* **1997**, *36*, 6409.

(12) (a) Jiang, H.-L.; Mao, J.-G. *Inorg. Chem.* **2006**, *45*, 717. (b) Nikiforov, G. B.; Kusainova, A. M.; Berdonosov, P. S.; Dolgikh, V. A.; Lightfoot, P. *J. Solid State Chem.* **1999**, *146*, 473. (c) Meier, S. F.; Schleid, T. *Z. Anorg. Allg. Chem.* **2003**, *629*, 1575.

(13) Wendlandt, W. M.; Hecht, H. G. *Reflectance Spectroscopy*; Interscience: New York, 1966.

(14) *Theory and Applications of Molecular Paramagnetism*; Boudreaux, E. A., Mulay, L. N., Eds.; John Wiley & Sons: New York, 1976.

(15) (a) Jiang, H. L.; Kong, F.; Fan, Y.; Mao, J. G. *Inorg. Chem.* **2008**, *47*, 7430. (b) Millet, P.; Enjalbert, R.; Galy, J. *J. Solid State Chem.* **1999**, *147*, 296.

Table 1. Crystal Data and Structure Refinements for the Title Compounds

	$Sr_2(VO)_3(SeO_3)_5$	$Sr(V_2O_5)(TeO_3)$	$Sr_2(V_2O_5)_2(TeO_3)_2(H_2O)$	$Ba_3(VO_2)_2(SeO_3)_4$	$Ba_2(VO_3)Te_4O_9(OH)$	$Ba_2V_2O_5(Te_2O_6)$
Fw	1010.86	445.10	908.22	1085.74	1045.03	807.76
space group	*Pnma*	$P\bar{1}$	*C*2/*c*	*P*2(1)/*n*	*P*2(1)/*n*	*P*2(1)/*m*
a/ Å	16.921(9)	10.196(4)	21.019(11)	8.953(3)	10.7661(7)	7.5076(9)
b/ Å	10.644(6)	11.085(5)	5.102(2)	15.445(5)	7.3084(3)	7.6687(8)
c/ Å	9.059(5)	13.995(6)	16.401(8)	11.464(3)	16.5883(14)	9.5710(12)
α/ deg	90	84.27(2)	90	90	90	90
β/ deg	90	70.453(15)	118.617(8)	92.462(5)	94.763(6)	93.568(13)
γ/ deg	90	73.136(16)	90	90	90	90
V/ Å^3	1631.4(15)	1426.5(10)	1544.1(12)	1583.9(8)	1300.71(15)	549.97(11)
Z	4	8	4	4	4	2
D_{calcd}/g cm^{-3}	4.116	4.145	3.907	4.553	5.337	4.878
μ(Mo-Kα)/mm^{-1}	19.403	14.032	12.972	17.757	15.549	13.956
GOF on F^2	1.077	1.061	0.894	1.029	1.050	1.091
R1, wR2[$I > 2\sigma(I)$][a]	0.0219, 0.0469	0.0330, 0.0633	0.0392, 0.0723	0.0360, 0.0680	0.0413, 0.0994	0.0259, 0.0607
R1, wR2(all data)	0.0254, 0.0482	0.0478, 0.0687	0.0627, 0.0834	0.0521, 0.0744	0.0442, 0.1015	0.0275, 0.0618

[a] $R1 = \sum||F_o| - |F_c||/\sum|F_o|$, $wR2 = \{\sum w(F_o^2 - F_c^2)^2/\sum w(F_o^2)^2\}^{1/2}$.

(23 mL) and heated at 230 °C for 4 days, followed by slow cooling to room temperature at a rate of 6 °C/h. The final pH values of the reaction media are close to 6.0 for both compounds. The EDS elemental analyses on several single crystals of $Sr(V_2O_5)(TeO_3)$ and $Sr_2(V_2O_5)_2(TeO_3)_2(H_2O)$ gave an average molar ratio of Sr/V/Te of 1.0:1.78:1.08 and 1.01:1.87:1.0, which is in good agreement with the one determined from single-crystal X-ray structural studies. The single phase of $Sr_2(V_2O_5)_2(TeO_3)_2(H_2O)$ was obtained in a yield of about 33% based on Sr. Its purity was confirmed by the XRD measurement (Supporting Information, Figure S1). The single phase of $Sr(V_2O_5)(TeO_3)$ was not obtained, and the main impurity is $Sr_2(V_2O_5)_2(TeO_3)_2(H_2O)$. Much effort was put into preparing the single phase of $Sr(V_2O_5)(TeO_3)$ by changing reaction temperatures, but it was unsuccessful; hence, its physical properties were not measured. We have try to convert $Sr_2(V_2O_5)_2(TeO_3)_2(H_2O)$ into $Sr(V_2O_5)(TeO_3)$ by removing the H_2O molecules. The residuals after heating $Sr_2(V_2O_5)_2(TeO_3)_2(H_2O)$ at 430 °C were characterized to be a mixed phase by X-ray diffraction; so, it can be supposed that the framework of $Sr_2(V_2O_5)_2(TeO_3)_2(H_2O)$ collapsed after the loss of H_2O molecule, and it can not transform.

Preparation of $Ba_3(VO_2)_2(SeO_3)_4$, $Ba_2(VO_3)Te_4O_9(OH)$, and $Ba_2V_2O_5(Te_2O_6)$. The three compounds were hydrothermally synthesized by reactions of a mixture of $Ba(OH)_2 \cdot 8H_2O$, V_2O_5 (or $NaVO_3 \cdot 2H_2O$), and SeO_2(or TeO_2) in 4 mL of distilled water at 230 °C for 4 days, followed by slow cooling to room temperature at a rate of 6 °C/h. For $Ba_3(VO_2)_2(SeO_3)_4$, the loaded compositions are $Ba(OH)_2 \cdot 8H_2O$ (0.3154 g, 1.0 mmol), V_2O_5 (0.0728 g, 0.4 mmol), and SeO_2 (0.1109 g, 1.0 mmol), and orange brick-shaped crystals of $Ba_3(VO_2)_2(SeO_3)_4$ along with some white powders were obtained. The final pH value of the reaction media is close to 2.0. For $Ba_2(VO_3)Te_4O_9(OH)$, the reaction mixtures were composed of $Ba(OH)_2 \cdot 8H_2O$ (0.1892 g, 0.6 mmol), V_2O_5 (0.0364 g, 0.2 mmol), and TeO_2 (0.1596 g, 1.0 mmol), and yellow brick-shaped crystals of $Ba_2(VO_3)Te_4O_9(OH)$ along with some gray powders were obtained. The final pH value of the reaction media is about 6.0. For $Ba_2V_2O_5(Te_2O_6)$, the mixtures were $Ba(OH)_2 \cdot 8H_2O$ (0.0946 g, 0.3 mmol), $NaVO_3 \cdot 2H_2O$ (0.1579 g, 1.0 mmol), TeO_2 (0.1596 g, 1.0 mmol), and H_2O (4 mL). The final pH value is 6.0. The EDS elemental analyses gave an average molar ratio of Ba/V/Se(Te) of 1.52:1.0:2.21, 1.96:1.0:3.86, and 1.15:1.0:1.08, which is in good agreement with the one determined from single-crystal X-ray structural studies. After proper structural analyses, these compounds were obtained as single phases by the reactions of a mixture of 0.3 mmol $Ba(OH)_2 \cdot 8H_2O$, 0.1 mmol V_2O_5, 0.4 mmol SeO_2 for $Ba_3(VO_2)_2(SeO_3)_4$; 0.4 mmol $Ba(OH)_2 \cdot 8H_2O$, 0.1 mmol V_2O_5, 0.8 mmol TeO_2 for $Ba_2(VO_3)Te_4O_9(OH)$; and 0.4 mmol $BaCO_3$, 0.2 mmol V_2O_5, and 0.4 mmol TeO_2 for $Ba_2V_2O_5(Te_2O_6)$ in 4 mL of H_2O at 230 °C for 4 days in a yield of about 74%, 39% and 48% respectively (based on Ba). Their purities were confirmed by XRD studies (Supporting Information, Figure S1).

X-ray Crystallography. Data collections for the above six compounds were performed on SATURN 70 CCD (for $Sr_2(VO)_3(SeO_3)_5$), SATURN 724 (for $Sr_2(V_2O_5)_2(TeO_3)_2(H_2O)$ and $Ba_3(VO_2)_2(SeO_3)_4$), and Rigaku SCXMini CCD (for three other compounds) diffractometers equipped with a graphite-monochromated Mo-Kα radiation ($\lambda = 0.71073$ Å) at 293 K. The data sets were corrected for Lorentz and polarization factors as well as for absorption by Multiscan method.[16a] All six structures were solved by direct methods and refined by full-matrix least-squares fitting on F^2 by SHELX-97.[16b] All non-hydrogen atoms were refined with anisotropic thermal parameters. The hydrogen atoms in $Ba_2(VO_3)Te_4O_9(OH)$ and $Sr_2(V_2O_5)_2(TeO_3)_2(H_2O)$ were located at calculated positions and refined with isotropic thermal parameters. Crystallographic data and structural refinements for the six compounds are summarized in Table 1. Important bond distances are listed in Table 2. More details on the crystallographic studies as well as atomic displacement parameters are given as Supporting Information.

Computational Descriptions. Single-crystal structural data of the six compounds were used for the theoretical calculations. The ab initio band structure calculations and density of states (DOS) were performed by using the computer code CASTEP.[17] The code employs density functional theory (DFT) using a plane wave basis set with Vanderbilt norm-conserving pseudopotentials to approximate the interactions between the core and valence electrons.[18] The exchange-correlation energy was calculated using the Perdew−Burke−Ernzerhof modification to the generalized gradient approximation (GGA).[19] The number of plane waves included in the basis set is determined by a kinetic-energy cutoff of 600 eV for $Sr_2(VO)_3(SeO_3)_5$, $Sr(V_2O_5)(TeO_3)$, $Sr_2(V_2O_5)_2(TeO_3)_2(H_2O)$ and 500 eV for $Ba_3(VO_2)_2(SeO_3)_4$, $Ba_2(VO_3)Te_4O_9(OH)$, and $Ba_2V_2O_5(Te_2O_6)$. The numerical integration of the Brillouin zone is performed by using $1 \times 2 \times 3$, $3 \times 2 \times 2$, $5 \times 5 \times 2$, $3 \times 2 \times 2$, $2 \times 3 \times 2$, and $3 \times 3 \times 3$ Monkhorst−Pack *k*-point sampling for the six compounds, respectively. Pseudoatomic calculations were performed for O

(16) (a) *CrystalClear*, Version 1.3.5; Rigaku Corp.: Woodlands, TX, 1999. (b) Sheldrick, G. M. *SHELXTL, Crystallographic Software Package*, Version 5.1; Bruker-AXS: Madison, WI, 1998.

(17) (a) Segall, M. D.; Lindan, P. J. D.; Probert, M. J.; Pickard, C. J.; Hasnip, P. J.; Clark, S. J.; Payne, M. C. *J. Phys.: Condens. Matter* **2002**, *14*, 2717. (b) Milman, V.; Winkler, B.; White, J. A.; Pickard, C. J.; Payne, M. C.; Akhmatskaya, E. V.; Nobes, R. H. *Int. J. Quantum Chem.* **2000**, *77*, 895.

(18) Lin, J. S.; Qteish, A.; Payne, M. C.; Heine, V. *Phys. Rev. B* **1993**, *47*, 4174.

(19) Perdew, J. P.; Burke, K.; Ernzerhof, M. *Phys. Rev. Lett.* **1996**, *77*, 3865.

Table 2. Important Bond Length (Å) for the Six Compounds[a]

$Sr_2(VO)_3(SeO_3)_5$[b]			
V(1)−O(9)	1.590(3)	V(1)−O(9)	1. 952(3)
V(1)−O(6) #1	2.007(3)	V(1)−O(1)	2.045(2)
V(1)−O(5)	2.126(3)	V(1)−O(4)	2.229(3)
V(2)−O(10)	1.597(4)	V(2)−O(2) #2	2.041(2)
V(2)−O(2) #3	2.041(2)	V(2)−O(3)	2.052(2)
V(2)−O(3) #4	2.052(2)	V(2)−O(8)#5	2.100(4)
Se(1)−O(1)	1.696(2)	Se(1)−O(3)	1.702(2)
Se(1)−O(2)	1.715(2)	Se(2)−O(4)	1.676(2)
Se(2)−O(6)	1.710(3)	Se(2)−O(5)	1.742(2)
Se(3)−O(8)	1.640(4)	Se(3)−O(7) #6	1.710(3)
Se(3)−O(7)	1.710(2)		
$Sr(V_2O_5)(TeO_3)$[c]			
V(1)−O(8)	1.609(4)	V(1)−O(9)	1.659(4)
V(1)−O(5)	1.954(4)	V(1)−O(1)	1.975(4)
V(1)−O(2)	2.014(4)	V(2)−O(10)	1.631(4)
V(2)−O(11)	1.668(3)	V(2)−O(3)	1.787(4)
V(2)−O(2) #1	1.789(4)	V(3)−O(12)	1.645(4)
V(3)−O(14)	1.650(4)	V(3)−O(4)	1.803(3)
V(3)−O(13)	1.807(4)	V(4)−O(16)	1.637(4)
V(4)−O(15)	1.661(4)	V(4)−O(7)	1.787(4)
V(4)−O(13) #2	1.820(4)	V(5)−O(24)	1.632(4)
V(5)−O(25)	1.666(3)	V(5)−O(18)	1.791(4)
V(5)−O(19) #3	1.806(4)	V(6)−O(27)	1.602(4)
V(6)−O(26)	1.663(4)	V(6)−O(23)	1.983(4)
V(6)−O(17)	1.989(3)	V(6)−O(18)	2.001(4)
V(7)−O(28)	1.638(4)	V(7)−O(29)	1.653(4)
V(7)−O(21)	1.789(4)	V(7)−O(31) #4	1.824(4)
V(8)−O(32)	1.646(4)	V(8)−O(30)	1.655(4)
V(8)−O(31)	1.794(4)	V(8)−O(20)	1.805(3)
Te(1)−O(1)	1.864(4)	Te(1)−O(3)	1.917(4)
Te(1)−O(4)	1.967(3)	Te(1)−O(2)	2.320(4)
Te(2)−O(6)	1.826(4)	Te(2)−O(5)	1.913(3)
Te(2)−O(7)	1.984(4)	Te(3)−O(17)	1.860(4)
Te(3)−O(19)	1.901(4)	Te(3)−O(20)	1.973(3)
Te(3)−O(18)	2.328(4)	Te(4)−O(22)	1.834(4)
Te(4)−O(23)	1.923(3)	Te(4)−O(21)	1.937(4)
$Sr_2(V_2O_5)_2(TeO_3)_2(H_2O)$[d]			
V(1)−O(4)	1.604(6)	V(1)−O(5)	1.636(5)
V(1)−O(6)	1.886(5)	V(1)−O(1)	1.974(5)
V(1)−O(1) #1	2.011(5)	V(2)−O(7)	1.640(5)
V(2)−O(8)	1.667(5)	V(2)−O(6)	1.726(6)
V(2)−O(2) #2	1.790(5)	Te(1)−O(3)	1.848(6)
Te(1)−O(2)	1.909(5)	Te(1)−O(1)	1.971(4)
$Ba_3(VO_2)_2(SeO_3)_4$			
V(1)−O(8)	1.636(5)	V(1)−O(7)	1.650(5)
V(1)−O(1)	1.905(5)	V(1)−O(5)	1.980(6)
V(1)−O(4)	1.993(6)	V(2)−O(18)	1.629(6)
V(2)−O(17)	1.636(5)	V(2)−O(14)	1.926(5)
V(2)−O(12)	2.028(5)	V(2)−O(11)	2.031(6)
Se(1)−O(3)	1.654(5)	Se(1)−O(2)	1.683(5)
Se(1)−O(1)	1.771(6)	Se(2)−O(6)	1.655(5)
Se(2)−O(5)	1.738(6)	Se(2)−O(4)	1.739(5)
Se(3)−O(13)	1.644(5)	Se(3)−O(12)	1.713(5)
Se(3)−O(11)	1.721(5)	Se(4)−O(15)	1.669(5)
Se(4)−O(16)	1.678(6)	Se(4)−O(14)	1.754(6)
$Ba_2(VO_3)Te_4O_9(OH)$[e]			
V(1)−O(13)	1.640(7)	V(1)−O(11)	1.688(8)
V(1)−O(12)	1.695(7)	V(1)−O(2)	1.875(6)
Te(1)−O(1)	1.817(6)	Te(1)−O(3)	1.890(6)
Te(1)−O(2)	1.927(6)	Te(2)−O(4)	1.839(6)
Te(2)−O(5)	1.949(6)	Te(2)−O(3)	2.109(6)
Te(2)−O(8)	2.157(6)	Te(3)−O(7)	1.834(6)
Te(3)−O(6)	1.874(6)	Te(3)−O(5)	2.021(6)
Te(4)−O(10)	1.835(6)	Te(4)−O(8)	1.921(6)
Te(4)−O(9)	2.021(6)	Te(4)−O(6)#1	2.244(6)
$Ba_2V_2O_5(Te_2O_6)$[f]			
V(1)−O(6)	1.630(5)	V(1)−O(5)	1.637(6)
V(1)−O(4)	1.804(4)	V(1)−O(4)#1	1.804(4)
V(2)−O(7)#2	1.663(4)	V(2)−O(7)	1.663(4)
V(2)−O(8)	1.725(5)	V(2)−O(3)	1.804(5)
Te(1)−O(2)	1.840(3)	Te(1)−O(1)	1.970(3)
Te(1)−O(4)	2.054(3)	Te(1)−O(3)	2.205(3)

[a] Symmetry transformations used to generate equivalent atoms are given in footnotes *b*−*f*. [b] For $Sr_2(VO)_3(SeO_3)_5$: #1 $-x+1/2, -y, z+1/2$; #2 $-x, y-1/2, -z+1$; #3 $-x, -y, -z+1$; #4 $x, -y-1/2, z$; #5 $-x, -y, -z+2$; #6 $x, -y+1/2, z$. [c] For $Sr(V_2O_5)(TeO_3)$: #1 $-x+1, -y, -z+1$; #2 $-x, -y+1, -z+1$; #3 $-x+1, -y, -z$; #4 $-x, -y+1, -z$. [d] For $Sr_2(V_2O_5)_2(TeO_3)_2(H_2O)$: #1 $-x+1/2, -y+1/2, -z$; #2 $x, -y+1, z-1/2$. [e] For $Ba_2(VO_3)Te_4O_9(OH)$: #1 $x, y+1, z$. [f] For $Ba_2V_2O_5(Te_2O_6)$: #1 $x, -y-1/2, z$; #2 $x, -y+1/2, z$.

$2s^22p^4$, Se $4s^24p^4$, Te $5s^25p^4$, V $3d^34s^24p^0$, Sr $4s^24p^65s^2$, Ba $5s^25p^66s^2$. Spin polarization of vanadium(IV) atom was included for the electronic structure calculations of $Sr_2(VO)_3(SeO_3)_5$. The other calculating parameters used in the calculations and convergent criteria were set by the default values of the CASTEP code.

Result and Discussion

Six new alkaline earth metal vanadium(V) or vanadium(IV) selenites and tellurites, namely, $Sr_2(VO)_3(SeO_3)_5$, $Sr(V_2O_5)(TeO_3)$, $Sr_2(V_2O_5)_2(TeO_3)_2(H_2O)$, $Ba_3(VO_2)_2(SeO_3)_4$, $Ba_2(VO_3)Te_4O_9(OH)$, and $Ba_2V_2O_5(Te_2O_6)$ have been prepared by hydrothermal reactions of $SrCO_3$ (or $Ba(OH)_2\cdot 8H_2O$ or $BaCO_3$), SeO_2 (or TeO_2), and V_2O_5 in different molar ratios at 230 °C. In $Sr_2(VO)_3(SeO_3)_5$, the V_2O_5 was reduced to +4 by excess SeO_2. When $Ba(OH)_2\cdot 8H_2O$ was used instead of $SrCO_3$, $Ba_3(VO_2)_2(SeO_3)_4$ with vanadium in an oxidation state of +5 was isolated. For the four vanadium tellurites, the vanadium and tellurium exhibit a different oligomer or infinite chain because of the different molar ratios of V_2O_5 and TeO_2. Hence, the different reactant ratios and the consequent pH values and concentrations play an important role in the chemical compositions and structures of the compounds formed. These six compounds display six different types of structures as will be discussed in the following sections.

Structural Descriptions. $Sr_2(VO)_3(SeO_3)_5$ is isostructural to $Pb_2(VO)_3(SeO_3)_5$ previously reported.[9] Its structure features a 3D anionic framework of $[(VO)_3(SeO_3)_5]^{4-}$ with 1D tunnels of 8-MRs along the *b*-axis which are filled by the Sr^{2+} ions (Figure 1a). There are two Sr^{2+} ions (both located on the mirror plane), two V^{4+} (one on the mirror plane and one at general position), three Se^{4+} atoms (two at general sites and one on the mirror plane) in the asymmetric unit. V(1) is octahedrally coordinated by one selenite anion in a bidentate chelating fashion, three selenite anions in a unidentate fashion, and a terminal oxygen whereas V(2) is octahedrally coordinated by five selenite anions in a unidentate fashion and one terminal oxygen. Both $V(1)O_6$ and $V(2)O_6$ octahedra are distorted toward a corner (local C_4 direction) with one "short" (1.590(3)−1.597(4) Å), four "normal" (1.952(3)−2.126(3) Å), and one "long" (2.100(4)−2.229(3) Å) V−O bonds (Table 2). Such type of distortion has also been reported in $ZnVSe_2O_7$, $VO(SeO_3)\cdot H_2O$,[15] $Cu(VO)(SeO_3)_2$, and mixed valence KV_2SeO_7.[20] The *trans* O−V−O bond angles fall in the range of 146.9(1)−178.6(2)° whereas the *cis* ones in the range of 69.1(1) to 102.3(1)°.

(20) (a) Lee, K.-S.; Kwon, Y.-U.; Namgung, H.; Kim, S.-H. *Inorg. Chem.* **1995**, *34*, 4178. (b) Huan, G.-H.; Johnson, J. W.; Jacobson, A. J.; Goshorn, D. P. *Chem. Mater.* **1991**, *3*, 539.

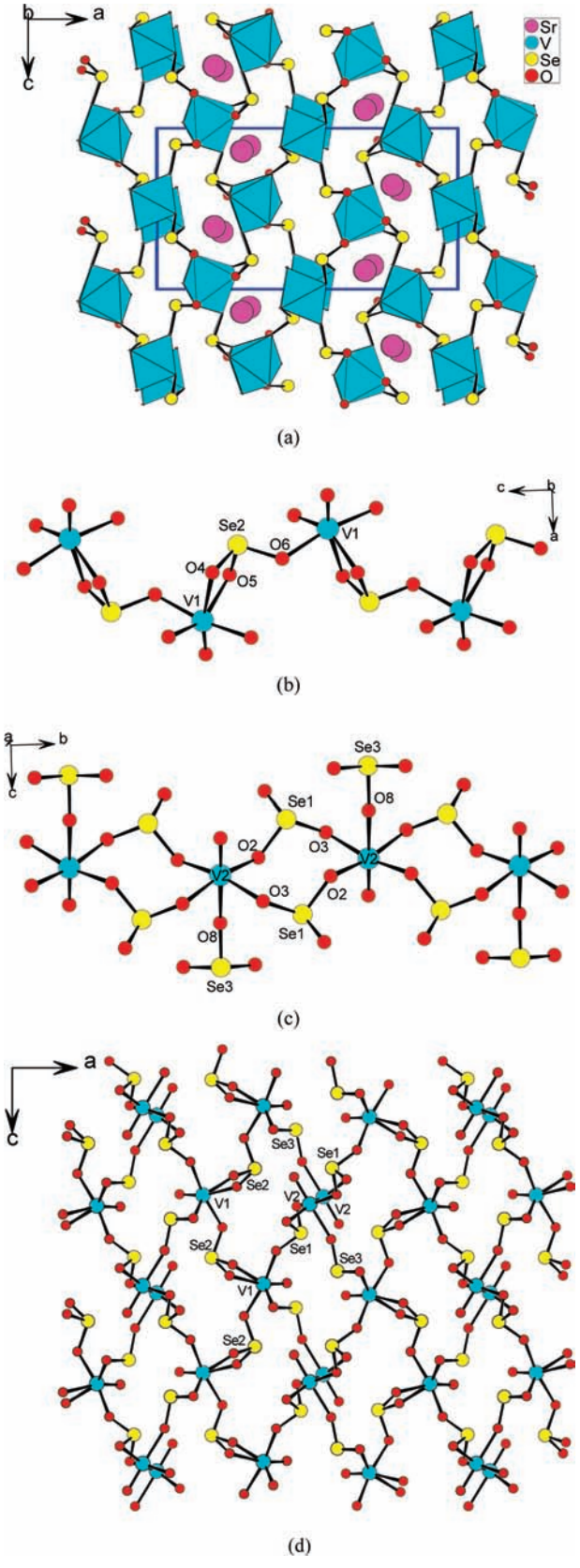

Figure 1. View of the structure of $Sr_2(VO)_3(SeO_3)_5$ along the *b*-axis (a), the vanadium(IV) selenite chains along *c*- (b), and *b*-axis (c), and the 3D anionic framework of $[(VO)_3(SeO_3)_5]^{4-}$ (d).

Taking into account the six V−O bond lengths and the three trans O−V−O bond angles, the magnitude of the distortion (Δd) was calculated to be 0.934 and 0.592 Å[21] for $V(1)O_6$ and $V(2)O_6$, which is comparable to that in $Pb_2V^{IV}{}_3Se_5O_{18}$.[9] The distortion is away from the lone pair cation Se(IV). All three Se(IV) cations are coordinated by three oxygen atoms in a distorted Ψ-SeO_3 trigonal-pyramidal geometry with the lone pair of Se(IV) occupying the pyramidal site. The Se−O distances fall in the normal range of 1.640(4)−1.742(2) Å (Table 2). BVS calculations indicate that all V and Se atoms are in oxidation states of +4. The calculated total bond valences for V(1), V(2), Se(1), Se(2), and Se(3) atoms are 4.277, 4.265, 4.003, 3.959, and 4.215, respectively.[22]

Neighboring $V(1)O_6$ octahedra are bridged by the $Se(2)O_3$ group via edge- (O(4) and O(5)) and corner-sharing (O(6)) into a 1D zigzag chain along the *c*-axis whereas two neighboring $V(2)O_6$ octahedra are bridged by a pair of $Se(1)O_3$ groups via corner-sharing (O(2) and O(3)) into a 1D chain along the *b*-axis with the $Se(3)O_3$ hanging on the chain (Figures 1b and 1c). The intra chain V···V distances are 5.380(3) and 5.475(2) Å, respectively, and those of the inter chain are in the range of 5.475(2)−6.173(2) Å. The intergrowth of the above chains results in an anionic framework with two types of 1D 8-MR tunnels running along the *b*-axis (Figure 1d). The lone pairs of Se atoms are oriented toward the vacant part of the tunnels, and the other part is filled by Sr^{2+} ions. The Sr^{2+} ions are surrounded by eight oxygen atoms in a distorted cubic geometry with the Sr−O distances ranging from 2.477(3) to 2.929 Å, which are comparable to those reported in other strontium compounds.[23]

It is interesting to compare the structures of $Sr_2(VO)_3(SeO_3)_5$ and $Ba(VO_2)(SeO_3)_2(HSeO_3)$.[10c] The two compounds exhibit different 3D anionic networks based on $V^{IV}O_6$ octahedra bridged by SeO_3 or/and $HSeO_3$ groups via corner-sharing. One selenite group in $Ba(VO_2)(SeO_3)_2(HSeO_3)$ is protonated and acts as a bidentate metal linker, and the barium(II) ions are located at 1D tunnels of 4-MRs.

The structure of $Sr(V_2O_5)(TeO_3)$ features novel vanadium(V) tellurite chains in which V_2O_7 and V_2O_8 dimers are bridged by TeO_4 and TeO_3 groups (Figure 2). The asymmetric unit of $Sr(V_2O_5)(TeO_3)$ contains four Sr^{2+}, eight V^{5+}, and four Te(IV) atoms. Both V(1) and V(6) are five-coordinated by five oxygen atoms from two tellurite groups and two oxo anions in a distorted square pyramidal environment with two "short" (1.602(4)−1.663(4) Å) and three "normal" (1.954(4)−2.014(4) Å) V−O bonds (Table 2) whereas the other six V^{5+} ions are tetrahedrally coordinated by four oxygen atoms in a distorted tetrahedral environment with V−O distances ranging from 1.631(4) to 1.824(4) Å (Table 2). V(5) and V(2) each connects with two TeO_4 groups whereas V(3), V(4), V(7), and V(8) each connects with only one TeO_3 or TeO_4 group. Both VO_5 square pyramids and VO_4 tetrahedra are significantly distorted. In VO_5 square pyramid, the *cis* O−V−O angles range from 75.78(15) to 110.7(2)° whereas the *trans* ones are in the range of 141.3(2) and 149.8(2)°; the O−V−O angles within the VO_4 tetrahedra are in the range of 99.45(17)−116.08 (17)°. It is noticed

(21) Halasyamani, P.-S. *Chem. Mater.* **2004**, *16*, 3586.
(22) (a) Guesdon, A.; Raveau, B. *Chem. Mater.* **2000**, *12*, 2239. (b) Chi, E. O.; Ok, K. M.; Porter, Y.; Halasyamani, P. S. *Chem. Mater.* **2006**, *18*, 2070.
(23) (a) Loureiro, S. M.; Felser, C.; Huang, Q.; Cava, R. J. *Chem. Mater.* **2000**, *12*, 3181. (b) Hector, A. L.; Hutchings, J.; Needs, R. L.; Thomas, M. F.; Weller, M. T. *J. Mater. Chem.* **2001**, *11*, 527.

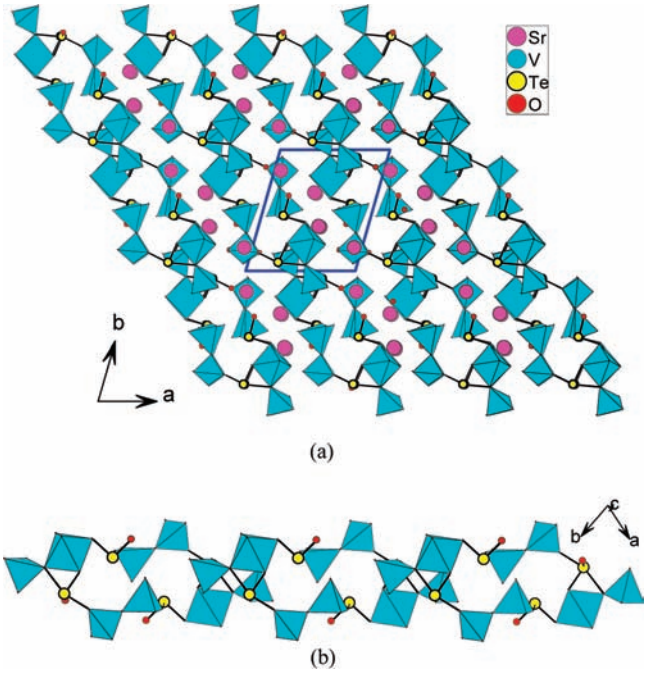

Figure 2. View of the structure of $Sr(V_2O_5)(TeO_3)$ along the *c*-axis (a), and a 1D vanadium(V) tellurite chain along the [2 2 0] direction (b).

that the "normal" V−O bonds are further bonded to other Te^{4+} or V^{5+} cations whereas the "short" V−O bonds remain terminal in VO_5 polyhedra. Among the four Te^{4+} cations in the asymmetric unit, Te(1) and Te(3) cations are four-coordinated in a "seesaw" geometry, displaying three "normal" Te−O bonds (1.860(4)−1.973(3) Å) and one "long" Te−O bonds (2.320(4)−2.328(4) Å). The O−Te−O angles range from 70.7(1)−158.1(2)° (Table 2). Both Te(2) and Te(4) cations are three-coordinated in distorted Ψ-TeO_3 tetrahedral geometry, with the fourth site occupied by the lone-pair electrons. The Te−O distances fall in the range of 1.826(4)−1.984(4) Å (Table 2). BVS calculations gave total bond valences of 5.024, 5.115, 5.034, 5.033 5.061, 4.987, 5.045, 5.040 for V(1)−V(8) atoms and 4.123, 4.221, 3.998, 4.149 for Te(1)−Te(4), indicating oxidation states of +5 and +4 for V and Te, respectively.[22]

$V(1)O_5$ and $V(2)O_4$ or $V(6)O_5$ and $V(5)O_4$ form a V_2O_8 dimer via corner-sharing whereas the remaining VO_4 tetrahedra form V_2O_7 dimers via corner-sharing. The V···V separations within V_2O_8 and V_2O_7 dimers are in the range of 3.434(1)−3.472(1) Å and 3.383(1)−3.385(1) Å, respectively. The above two types of dimers are bridged by TeO_3 and TeO_4 groups into 1D chains in the [2 2 0] direction, forming alternative V_2Te_2 4-MRs and V_6Te_4 10-MRs (Figure 2c). The TeO_3 group is bridged to one V_2O_7 and one V_2O_8 dimers whereas the TeO_4 group is bridged to one V_2O_7 and two V_2O_8 dimers. The Sr^{2+} ions are located at the interchain space. The $Sr(1)^{2+}$ and $Sr(4)^{2+}$ ions are nine-coordinated in a tricapped trigonal prism geometry whereas the $Sr(2)^{2+}$ and $Sr(3)^{2+}$ ions are eight-coordinated in a bicapped trigonal prism geometry. The Sr−O distances are in the range of 2.403(4) and 3.018(4) Å, which are close to those in $Sr_2(VO)_3(SeO_3)_5$.

It is worthy of note that the structure of $Sr(V_2O_5)$-(TeO_3) differs from that of BaV_2TeO_8 with a similar chemical formula.[10a] The latter features a 1D chain composed of VO_4 tetrahedra and dimers of edge-sharing VO_5

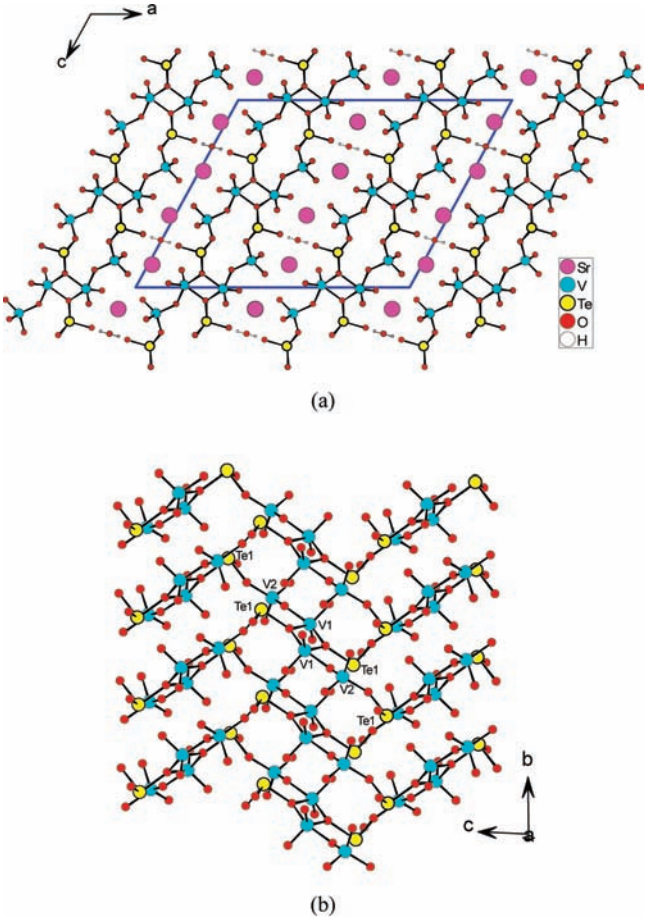

Figure 3. View the structure of $Sr_2(V_2O_5)_2(TeO_3)_2(H_2O)$ down the *b*-axis (a) and a vanadium(V) tellurite layer parallel to the *bc* plane (b).

square pyramids bridged by solely TeO_4 groups, forming 8-MRs composed of two VO_4 tetrahedra, two VO_5 square pyramids, and four TeO_4 groups.

The structure of $Sr_2(V_2O_5)_2(TeO_3)_2(H_2O)$ features a 2D layer consisting of linear $[V_4O_{14}]$ tetramers bridged by TeO_3^{2-} anions with Sr^{2+} ions and water molecules located at the interlayer space (Figure 3a). The asymmetric unit of $Sr_2(V_2O_5)_2(TeO_3)_2(H_2O)$ contains one Sr^{2+}, two V^{5+}, one Te^{4+} atoms. The V(1) atom is bonded to two tellurite oxygens from two tellurite groups, one bridging and two terminal oxo anions in a distorted trigonal bipyramidal geometry whereas the V(2) atom is tetrahedrally coordinated by one tellurite anion, one bridging and two terminal oxo anions. The V−O bonds distances range from 1.604(6) to 2.011(5) Å (Table 2). Within the $V(1)O_5$, the two terminal V−O bonds are short (1.604(6) and 1.636(5) Å) and the V−O bond of the V−O−V bridge is 1.886(5) Å whereas the V−O bonds of the V−O−Te bridges are 1.974(5) and 2.011(5) Å. The V−O bond distances within the $V(2)O_4$ are 1.640(5) and 1.667(5) Å for the two terminal V−O bonds, 1.726(6) Å for that of V−O−V bridge and 1.790(5) Å for that of the V−O−Te. The O−V−O angles within $V(1)O_5$ and $V(2)O_4$ are also different. The O−V−O angles within the $V(1)O_5$ range from 72.3(2) to 152.9(2)° whereas those of $V(2)O_4$ fall in the range of 104.0(3)−114.0(3)°. The tellurium(IV) atom is three-coordinated in a distorted Ψ-TeO_3 tetrahedral geometry, with the fourth site occupied by the lone-pair electrons. The Te−O distances fall in the

range of 1.848(6)−1.971(4) Å with the O−Te−O angles in the range of 92.1(2) and 95.2(2)°, which is typical for TeO_3 group (Table 2). The terminal O(3) atoms of the tellurite groups and the water molecule formed interlayer hydrogen bondings. The distance between the O(3) and O(1)W is 2.777(2) Å and the corresponding O(3)−H(1)WA−O(1)W angle is 144.67(2)°, indicating the existence of the hydrogen bonding. The BVS calculations indicate that the V and Te atoms are in oxidation states of +5 and +4. The calculated total bond valences for V(1), V(2), and Te(1) are 5.282, 5.265, and 3.874, respectively.[22]

A pair of the $V(1)O_5$ form a V_2O_8 dimer via edge-sharing (two O(1) corners). The V_2O_8 dimer is attached by one $V(2)O_4$ tetrahedron via corner-sharing on each side so as to form a linear $[V_4O_{14}]$ tetramer. The V···V distances within the tetramer range from 3.217(3) to 3.356(5) Å. Neighboring $[V_4O_{14}]$ clusters are bridged by TeO_3^{2-} groups via V−O−Te bridges into a 2D layer in the *bc* plane (Figure 3b). The interlayer *d*-spacing is about 10.18 Å. The tellurite group is tridentate and bridges with one VO_4 tetrahedron and two VO_5 trigonal bipyramids. The Sr^{2+} ions and water molecules are located at the interlayer space. The Sr^{2+} ion are eight-coordinated by eight atoms from two VO_5, three VO_4, two TeO_3 groups, and one aqua ligand in bicapped trigonal prism with Sr−O distances in the range of 2.495(5) and 2.819(6) Å.

$Ba_3(VO_2)_2(SeO_3)_4$ exhibits 0D $[(VO_2)(SeO_3)_2]^{3-}$ anions that are separated by Ba^{2+} ions (Figure 4a). There are three Ba^{2+}, two VO_2^+, and four SeO_3^{2-} anions in the asymmetric unit. Both V^{5+} are five-coordinated by three oxygens from two selenite anions and two terminal oxygen atoms in a trigonal bipyramidal geometry, displaying three "normal" (1.905(5)−2.031(6) Å) and two "short" (1.629(6)−1.650(5) Å) V−O bonds (Table 2). The O−V−O angles are in the range from 73.6(2) to 154.0(2)°. Hence the VO_5 trigonal bipyramids are significantly distorted. All four Se(IV) cations are three-coordinated by three oxygen atoms in a distorted Ψ-SeO_3 trigonal-pyramidal geometry with the lone pair of Se(IV) occupying the pyramidal site. The Se−O distances fall in the normal range of 1.644(5)−1.771(6) Å (Table 2). BVS calculations indicate that the V and Se atoms are in oxidation states of +5 and +4. The calculated total bond valences for V(1), V(2), Se(1), Se(2), Se(3), and Se(4) atoms are 5.060, 4.972, 4.056, 3.975, 4.149, and 4.067, respectively.[22]

Each VO_5 square pyramid is connected to a SeO_3^{2-} anion through edge-sharing and a second selenite group via corner-sharing, resulting in the formation of a 0D $[(VO_2)(SeO_3)_2]^{3-}$ anion (Figure 4b). Within the $[(VO_2)(SeO_3)_2]^{3-}$ anion, one selenite anion is bidentate chelating whereas the other one is unidentate. The Ba^{2+} ions are located between these $[(VO_2)(SeO_3)_2]^{3-}$ anions. Ba(1) and Ba(2) ions are eleven-coordinated whereas the $Ba(3)^{2+}$ ion is ten-coordinated and the Ba−O distances fall in the range of 2.682(5)−3.149(6) Å, which are comparable to those reported in $Ba(VO_2)(SeO_3)_2(HSeO_3)$.[10c]

It is interesting to note that both $Ba_3(VO_2)_2(SeO_3)_4$ and $Ba_{2.5}(VO_2)_3(SeO_3)_4\cdot H_2O$ are structurally based on VO_5 and SeO_3 polyhedra, but their structures are quite different.[10b] $Ba_{2.5}(VO_2)_3(SeO_3)_4\cdot H_2O$ features a layered structure in which VO_5 polyhedra are interconnected by both bidentate and tridentate SeO_3 groups, forming

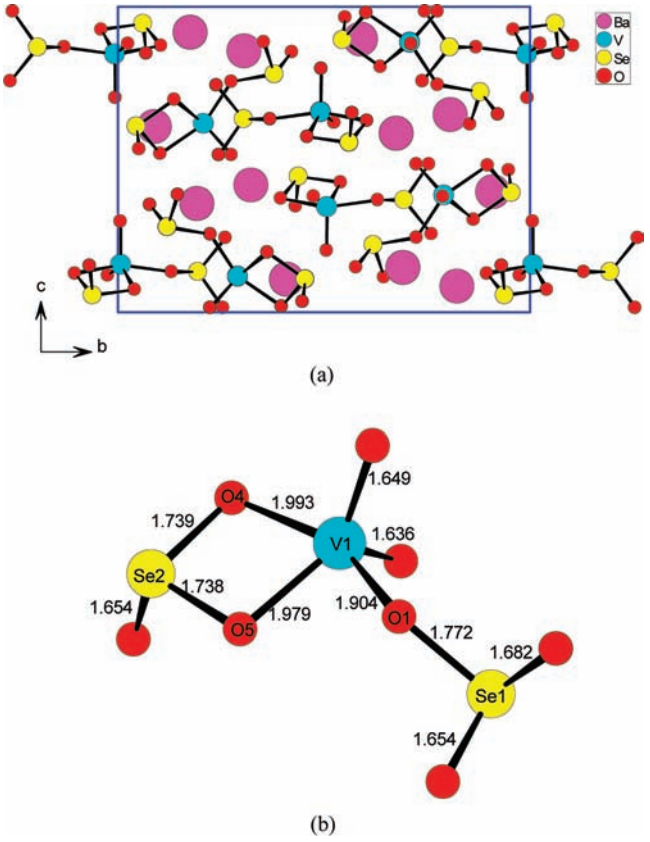

Figure 4. View the structure of $Ba_3(VO_2)_2(SeO_3)_4$ down the *a*-axis (a) and a $[(VO_2)(SeO_3)_2]^{3-}$ anion with bond distances labeled (b).

V_4Se_4 8-MRs and V_6Se_6 12-MRs. In $Ba_3(VO_2)_2(SeO_3)_4$, two selenite anions are bidentate chelating whereas the other two are unidentate; hence the compound has a much lower dimensionality.

$Ba_2(VO_3)Te_4O_9(OH)$ exhibit a novel 1D $[Te_4O_9(OH)]^{3-}$ chain decorated by VO_4 tetrahedra with the Ba^{2+} located at the interchain space (Figure 5a). The asymmetric unit of $Ba_2(VO_3)Te_4O_9(OH)$ contains two Ba^{2+}, one V^{5+}, and four Te^{4+} atoms. The V^{5+} is tetrahedrally coordinated by three terminal oxo anions and one tellurite oxygen atom with the V−O distances ranging from 1.640(7) to 1.875(6) Å (Table 2). It is noticed that the terminal V−O bonds of 1.640(7) to 1.695(7) Å are significantly shorter than the V−O bond of the V−O−Te bridge (1.875(6) Å). The O−V−O angles fall in the range of 104.7(3) and 114.2(4)°. Both Te(1) and Te(3) cations are three-coordinated in distorted Ψ-TeO_3 tetrahedral geometry, with the fourth site occupied by the lone-pair electrons. The Te−O distances fall in the normal range of 1.817(6)−2.021(6) Å (Table 2). The Te(2) and Te(4) cations are four-coordinated by four oxygen atoms in a "seesaw" geometry with the Te−O distances from 1.835(6) to 2.244(6) Å (Table 2). The O−Te−O angles of the TeO_3 groups are in the range of 89.9(3)−100.8(3)° whereas those of the TeO_4 groups fall in the range of 77.2(2)−163.8(2)°. It is also noticed that O(9) is protonated with Te−O distance of 2.012 Å. The O(9) atoms of the tellurites groups and the terminal O(13) atoms of $V(1)O_4$ polyhedra in neighboring chains formed interchain hydrogen bondings. The distance between the O(9) and O(13) is 2.914(3) Å and the corresponding O(9)−H(9A)−O(13) angle is 157.54(0)°, which is in the normal range for a

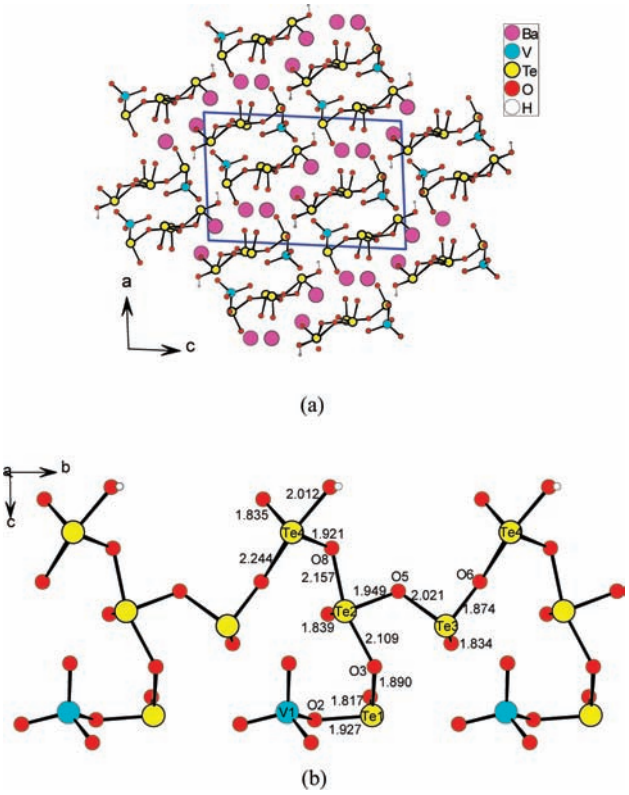

Figure 5. View the structure of $Ba_2(VO_3)Te_4O_9(OH)$ down the *b*-axis (a) and the 1D $[(VO_3)Te_4O_9(OH)]^{4-}$ chain along the *b*-axis (b).

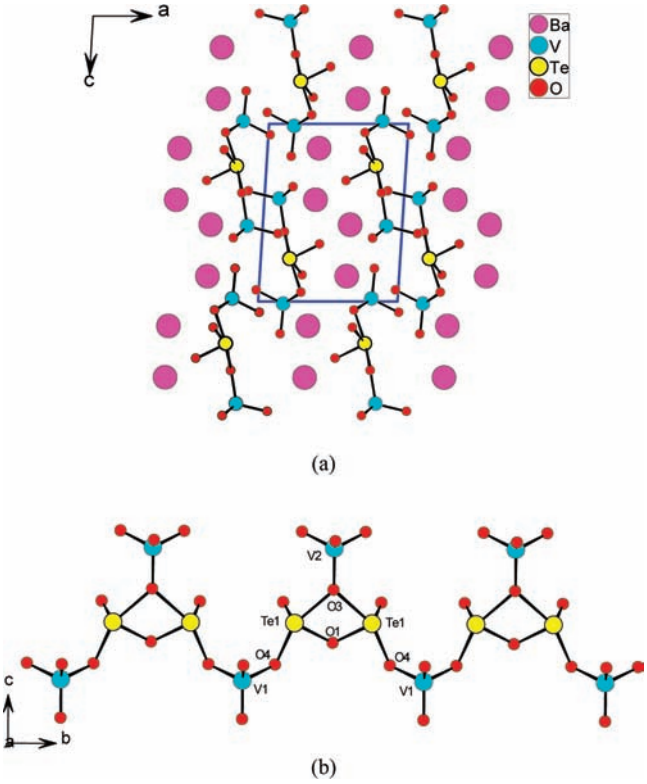

Figure 6. View the structure of $Ba_2V_2O_5(Te_2O_6)$ down the *b*-axis (a) and the 1D $[V_2O_5(Te_2O_6)]^{4-}$ chain along the *b*-axis (b).

hydrogen-bond. Bond valence calculations indicate that V and Te atoms are in oxidation states of +5 and +4. The calculated total bond valences for the V(1), Te(1), Te(2), Te(2), and Te(4) atoms are 5.080, 3.951, 3.845, 3.907, and 4.027, respectively.[22]

$Te(2)O_4$ and $Te(4)O_4$ groups form a Te_2O_7 dimer via corner-sharing (O(8)), such dimers are further bridged by $Te(3)O_3$ polyhedra via corner-sharing (O(5) and O(6)) into a 1D tellurium(IV) oxide chain along the *b*-axis. The $Te(1)O_3$ groups are hanging on the same side of the chain through Te(1)−O(3)−Te(2) bridges, resulting in a 1D $[Te_4O_9(OH)]^{3-}$ chain (Figure 5b). The discrete VO_4 tetrahedra are attached on the $Te(1)O_3$ groups via corner-sharing with Te−O−V angle of 121.8(3)°.

The 1D $[Te_4O_9(OH)]^{3-}$ anionic chain is quite different from the 0D $[Te_4O_{11}]^{6-}$ anion[24] and the 1D $[Te_4O_{10}]^{4-}$ anionic chain[7b] although they have similar compositions. In $[Te_4O_{11}]^{6-}$, two $Te(1)O_4$ polyhedra are interconnected via corner-sharing to form a dimeric unit, and the latter is corner-sharing with two $Te(2)O_3$ polyhedra. In $[Te_4O_{10}]^{4-}$, $Te(3)O_4$ and $Te(4)O_3$ groups are interconnected via corner-sharing, leading to a linear chain with a dimer formed by $Te(1)O_3$ and $Te(2)O_4$ through corner-sharing hanging on the same side of the linear chain. Hence, the differences can be attributed to the different chelating fashion of TeO_x ($x = 3, 4$).

Ba^{2+} ions are located at the interchain space. Ba(1) is nine-coordinated by nine oxygen atoms from four TeO_3 and three TeO_4 groups (two of TeO_4 groups are in a bidentate chelating fashion) whereas Ba(2) is ten-coordinated by nine tellurite oxygen atoms and one oxygen from a VO_4 tetrahedron. The Ba−O distances fall in the range of 2.714(6)−3.088(6) Å, which are comparable to those reported in other related compounds.[10]

The structure of $Ba_2V_2O_5(Te_2O_6)$ features a 1D vanadium(V) tellurites chain in which the VO_4 tetrahedra are interconnected by the $[Te_2O_6]^{4-}$ dimers with the Ba^{2+} ions acting as the charge balancing cations (Figure 6a). The asymmetric unit of $Ba_2V_2O_5(Te_2O_6)$ contains two Ba^{2+} and two V^{5+} (both on the mirror plane) and one Te^{4+} atoms. Both V(1) and V(2) atoms are in a slightly distorted tetrahedral environment. V(1) is coordinated by two oxygen atoms from two tellurite groups and two terminal oxygen atoms, whereas V(2) is bonded to one oxygen atom from a tellurite group and three terminal oxygen atoms. The V−O distances fall in the range of 1.630(5) and 1.804(5) Å, and the O−V−O bond angles are in the range of 102.5(2)−113.1(2)° (Table 2). The Te(IV) atoms is four-coordinated with three "normal" (1.840(3)−2.054(3) Å) and one "long" Te−O bonds (2.205(3) Å) in a "seesaw" geometry (Table 2). The O−Te−O angles fall in the range of 73.4(2)−153.9(1)°. BVS calculations indicate that the V and Te atoms are in oxidation states of +5 and +4. The calculated total bond valences for V(1), V(2), and Te(1) are 5.157, 5.152, and 3.819, respectively.[22]

A pair of TeO_4 tetrahedra are interconnected into a $[Te_2O_6]^{4-}$ anion via edging-sharing (O(1) and O(3)). $V(1)O_4$ tetrahedra are bridged by $[Te_2O_6]^{4-}$ anions into a 1D zigzag chain along the *b*-axis. The $V(2)O_4$ tetrahedra are grafted into the chain on the same side (Figure 6b). Each $[Te_2O_6]^{4-}$ anion acts as a tridentate ligand and

(24) (a) Castro, A.; Enjalbert, R.; Lloyd, D.; Rasines, I.; Galy, J. *J. Solid State Chem.* **1990**, *85*, 100. (b) Ijjaali, I.; Flaschenriem, C.; Ibers, J. A. *J. Alloys Compd.* **2003**, *354*, 115. (c) Weber, F. A.; Meier, S. F.; Schleid, T. *Z. Anorg. Allg. Chem.* **2001**, *627*, 2225. (d) Shen, Y. L.; Mao, J. G. *J. Alloys Compd.* **2004**, *385*, 86.

bridges to three $V(1)O_4$ tetrahedra. This type of chain has not been reported before.

The Ba^{2+} ions are located at the interchain space as charge balancing cations. Ba(1) is eight-coordinated by four tellurite oxygens and four oxygens from four VO_4 tetrahedra in a bicapped trigonal prism geometry whereas Ba(2) is ten-coordinated by seven oxygen atoms from three $[Te_2O_6]^{4-}$ anions and three oxygen atoms from two VO_4 tetrahedra in a bicapped antiprism geometry. The Ba−O distances are in the range of 2.688(5)−3.057(3) Å, which are close to those $Ba_3(VO_2)_2(SeO_3)_4$, $Ba_2(VO_3)Te_4O_9(OH)$ and other related compounds.[10]

Optical Properties. The infrared spectra of $Sr_2(VO)_3(SeO_3)_5$, $Sr_2(V_2O_5)_2(TeO_3)_2(H_2O)$, $Ba_3(VO_2)_2(SeO_3)_4$, $Ba_2(VO_3)Te_4O_9(OH)$, and $Ba_2V_2O_5(Te_2O_6)$ display similar features (Supporting Information, Figure S2). The bands associated with the Se−O, Te−O, and V−O vibrations appeared between 400 and 1000 cm^{-1}. The bands between 850 and 1000 cm^{-1} as well as the bands around 610−760 cm^{-1} can be assigned to ν(V=O) or ν(V−O−V) and ν(V−O) vibrations, whereas Se(Te)−O and Se(Te)−O−Se(Te) vibrations are observed at the bands about 760−850 and 500−610 cm^{-1}. The peaks from 400 to 460 cm^{-1} may be ascribed to Te−O−V or Se−O−V vibrations. For $Sr_2(V_2O_5)_2(TeO_3)_2(H_2O)$, the bands at 3420 and 1640 cm^{-1} can be assigned to ν(H−O−H) and ν(O−H). The infrared vibrations and assignments are listed in the Supporting Information, Table S2. All of the assignments are consistent with those previously reported.[9,10b,25]

Optical reflectance spectrum measurements indicate that the band gaps of $Sr_2(VO)_3(SeO_3)_5$, $Sr_2(V_2O_5)_2(TeO_3)_2(H_2O)$, $Ba_3(VO_2)_2(SeO_3)_4$, $Ba_2(VO_3)Te_4O_9(OH)$, and $Ba_2V_2O_5(Te_2O_6)$ are approximately 2.47, 2.52, 2.87, 2.80, and 3.16 eV, respectively (Supporting Information, Figure S3). Hence, all six compounds can be considered as wide-band gap semiconductors.

TGA. TGA under a nitrogen atmosphere indicate that $Sr_2(VO)_3(SeO_3)_5$, $Sr_2(V_2O_5)_2(TeO_3)_2(H_2O)$, $Ba_3(VO_2)_2(SeO_3)_4$, $Ba_2(VO_3)Te_4O_9(OH)$, and $Ba_2V_2O_5(Te_2O_6)$ are stable up to 415, 380, 325, 765, and 810 °C, respectively (Figure 7).

$Sr_2(VO)_3(SeO_3)_5$ exhibit one main step of weight loss in the temperature range of 415−700 °C, and $Ba_3(VO_2)_2(SeO_3)_4$ exhibits three steps of weight losses in the temperature range of 325−1100 °C. The weight loss corresponds to the release of 5 mol of SeO_2 or 4 mol of SeO_2 per formula unit. The observed weight loss of 54.6% for $Sr_2(VO)_3(SeO_3)_5$ is close to the calculated one (54.9%) whereas the observed weight loss of 43.1% for $Ba_3(VO_2)_2(SeO_3)_4$ is slightly larger than the calculated one (40.9%). Powder XRD studies indicate that the residuals of $Sr_2(VO)_3(SeO_3)_5$ heated at 700 °C are amorphous.

$Sr_2(V_2O_5)_2(TeO_3)_2(H_2O)$ exhibits two main steps of weight loss, which can be attributed to the release of H_2O and TeO_2 molecules, respectively. The first step of weight loss in the temperature range 380−425 °C corresponds to the release of 1 mol of H_2O per formula unit.

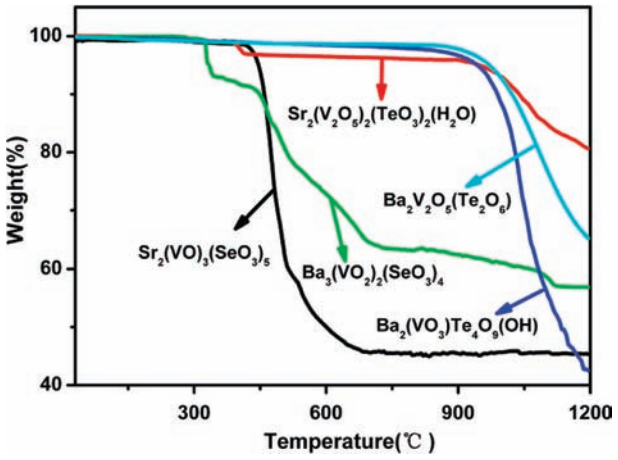

Figure 7. TGA diagrams for $Sr_2(VO)_3(SeO_3)_5$, $Sr_2(V_2O_5)_2(TeO_3)_2(H_2O)$, $Ba_3(VO_2)_2(SeO_3)_4$, $Ba_2(VO_3)Te_4O_9(OH)$, and $Ba_2V_2O_5(Te_2O_6)$.

The observed weight loss of 2.1% is close to the calculated one (2.0%). The second step of weight loss in the temperature range 890−1200 °C corresponds to the release of TeO_2. The observed total weight loss at 1200 °C is 19.4%. $Ba_2(VO_3)Te_4O_9(OH)$ and $Ba_2V_2O_5(Te_2O_6)$ exhibit one main step of weight loss which can be attributed to the release of TeO_2 (or and H_2O) molecules. The total weight losses at 1200 °C are about 57.5% and 34.7%, respectively, for $Ba_2(VO_3)Te_4O_9(OH)$ and $Ba_2V_2O_5(Te_2O_6)$. From the slope of the curve, it is clear that the decomposition is not complete at 1200 °C. The final residuals for all five compounds were not characterized because of their melting with the TGA bucket made of Al_2O_3 under such high temperature.

Magnetic Measurement. The temperature-dependent magnetic susceptibilities of $Sr_2(VO)_3(SeO_3)_5$ were measured at 1000 Oe in the temperature range 2−300 K since it contains paramagnetic V^{4+} ions (d^1).

$Sr_2(VO)_3(SeO_3)_5$ obeys the Curie−Weiss Law in the temperature range 20−300K (Figure 8). At 300 K, the $\chi_M T$ value is 1.01 emu·mol^{-1}·K, which is very close to the expected value of 1.125 emu·mol^{-1}·K for three V^{4+} ions per formula unit. The $\chi_M T$ value decreases continuously upon cooling and reaches a value of 0.053 emu·mol^{-1}·K at 2.0 K. A linear fit of the magnetic data in the range of 20−300 K gave a Weiss constant (θ) of −14.8 K, indicating antiferromagnetic interactions between the V^{4+} centers.[26] It is expected that the magnetic interaction occurred mainly between the V^{4+} centers interconnected by V−O−Se−O−V bridges with the V···V separations in the range of 5.380(3)−6.173(2) Å.

Theoretical Studies. The calculated band structures of the six compounds along high symmetry points of the first Brillouin zone are plotted in the Supporting Information, Figure S4. The state energies (eV) of the lowest conduction band (L-CB) and the highest valence band (H-VB) of the compounds are listed in the Supporting Information, Table S1. For $Sr_2(VO)_3(SeO_3)_5$, both the lowest of the CBs and the highest of the VBs are located at the G point

(25) (a) Lu, Y.; Wang, E. B.; Yuan, M.; Luan, G. Y.; Li, Y. G.; Zhang, H.; Hu, C. W.; Yao, Y. G.; Qin, Y. Y.; Chen, Y. B. *J. Chem. Soc., Dalton Trans.* **2002**, 3029. (b) Xiao, D. R.; Wang, S. T.; Wang, E. B.; Hou, Y.; Li, Y. G.; Hu, C. W.; Xu, L. *J. Solid State Chem.* **2003**, *176*, 159.

(26) (a) Berrocal, T.; Mesa, J. L.; Pizarro, J. L.; Bazan, B.; Iglesias, M.; Vilas, J. L.; Rojoa, T.; Arriortua, M. I. *Dalton Trans.* **2010**, *39*, 834. (b) Aldous, D. W.; Goff, R. J.; Attfield, J. P.; Lightfoot, P. *Inorg. Chem.* **2007**, *46*, 1277. (c) Kim, S.-H.; Halasyamani, P. S.; Melot, B. C.; Seshadri, R.; Green, M. A.; Sefat, A. S.; Mandrus, D. *Chem. Mater.* **2010**, *22*, 5074.

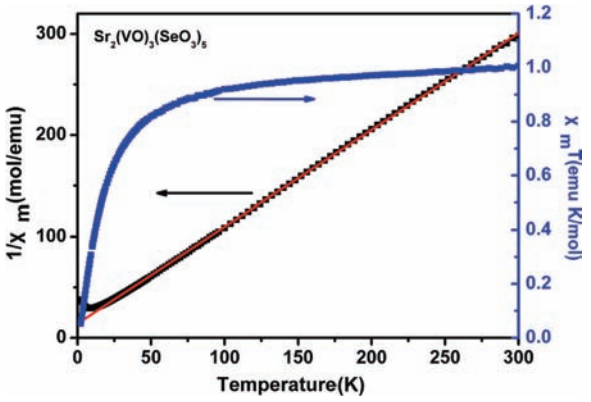

Figure 8. Plots of $1/\chi_m$ (black) and $\chi_m T$ (blue) versus T for $Sr_2(VO)_3(SeO_3)_5$. The red thin line represents the fitting according to the Curie–Weiss Law.

giving a direct band gap of 1.77 eV. For $Sr(V_2O_5)(TeO_3)$, $Sr_2(V_2O_5)_2(TeO_3)_2(H_2O)$, $Ba_3(VO_2)_2(SeO_3)_4$, $Ba_2(VO_3)Te_4O_9(OH)$, and $Ba_2V_2O_5(Te_2O_6)$, the lowest of the CBs and the highest of the VBs are located at different symmetry points. They revealed indirect band-gaps of 2.65, 2.54, 2.65, 2.84, and 3.15 eV, respectively.

The calculated band gaps for $Sr_2(VO)_3(SeO_3)_5$, $Sr_2(V_2O_5)_2(TeO_3)_2(H_2O)$, $Ba_3(VO_2)_2(SeO_3)_4$, $Ba_2(VO_3)Te_4O_9(OH)$, and $Ba_2V_2O_5(Te_2O_6)$ are somehow different from the experimental values (2.47, 2.52, 2.87, 2.80, and 3.16 eV, respectively). This is not surprising because it is well-known that GGA does not accurately describe the eigenvalues of the electronic states. The quantitative underestimation[27] or overestimation[28] of band gaps by the DFT calculations has also been reported for other inorganic compounds.

The bands can be assigned according to the total and partial densities of states (DOS) as plotted in the Supporting Information, Figure S5. Since all of the six compounds display similar characteristics, we only take $Sr(V_2O_5)(TeO_3)$ as a representative to discuss the DOS in detail. The bottom-most VB region around −31.5 eV comes from Sr-4s, 5s states. The bands between −19 and −13 eV mainly originated from O-2s states and Sr-4p states. Te-5s and O-2p states contribute to the energy region of −10 to −7.5 eV. In the Fermi level regions, namely, −6 to 0 eV in VB and 2.6 to 5 eV in CB, the overlaps of O-2p and V-3d or Se-4p (or Te-5p) indicate the well-defined V−O coordination in vanadium oxide polyhedra and Se−O (or Te−O) covalent interactions. When the spin splitting near the Fermi level is inspected, a small splitting is observed in $Sr_2(VO)_3(SeO_3)_5$, which is in good agreement with the effective magnetic moment from the magnetic measurements.

In addition, the bond orders of Sr−O (or Ba−O), Se−O (or Te−O), and V−O bonds in the six compounds have been calculated. The calculated bond orders of Sr−O bonds are 0.02−0.08, 0.02−0.10, and 0.01−0.08 e, respectively for $Sr_2(VO)_3(SeO_3)_5$, $Sr(V_2O_5)(TeO_3)$, and $Sr_2(V_2O_5)_2(TeO_3)_2(H_2O)$ whereas the calculated bond orders of Ba−O bonds are 0.02−0.10, 0.03−0.09, and 0.04−0.11 e, for $Ba_3(VO_2)_2(SeO_3)_4$, $Ba_2(VO_3)Te_4O_9(OH)$, and $Ba_2V_2O_5(Te_2O_6)$. The calculated bond orders of Se−O bonds are 0.34−0.50 e for Se−O(-V) bonds in $Sr_2(VO)_3(SeO_3)_5$ whereas the bond orders of Se−O(terminal) bonds and Se−O(-V) bridges in $Ba_3(VO_2)_2(SeO_3)_4$ are 0.40−0.51 and 0.21−0.36 e, respectively. The Te−O bonds in TeO_3 and TeO_4 groups exhibit different characteristic bond orders. In $Sr(V_2O_5)(TeO_3)$, the calculated bond orders were 0.12−0.53 e for the TeO_4 groups, and those of TeO_3 groups are in the range of 0.31−0.60 e. In $Sr_2(V_2O_5)_2(TeO_3)_2(H_2O)$, the Te−O bond orders (all TeO_3) are in the range of 0.24−0.58 e. In $Ba_2(VO_3)Te_4O_9(OH)$, the calculated bond orders were 0.21−0.52 e for the TeO_3 groups and those of TeO_4 groups are in the range of 0.08−0.59 e. In $Ba_2V_2O_5(Te_2O_6)$, the Te−O bond orders are in the range of 0.07−0.57 e. The V−O bonds can be divided into three types: V−O(terminal), V−O(-Se or Te), and V−O(-V). The calculated bond orders of V−O(terminal) are 0.94, 0.83−0.92, 0.77−0.90, 0.79−0.88, 0.75−0.87, and 0.70−0.89 e; and those of the V−O−Se (or Te) bridges are 0.18−0.50, 0.32−0.37, 0.28−0.30, 0.31−0.39, 0.43, and 0.53, respectively for $Sr_2(VO)_3(SeO_3)_5$, $Sr(V_2O_5)(TeO_3)$, $Sr_2(V_2O_5)_2(TeO_3)_2(H_2O)$, $Ba_3(VO_2)_2(SeO_3)_4$, $Ba_2(VO_3)Te_4O_9(OH)$, and $Ba_2V_2O_5(Te_2O_6)$. The V−O bond orders of the V−O−V bridges in $Sr(V_2O_5)(TeO_3)$ and $Sr_2(V_2O_5)_2(TeO_3)_2(H_2O)$ are 0.52−0.62 and 0.41−0.62 e, respectively.

It is noticed that the covalent character of the V−O bond is normally larger than that of the Se−O or Te−O bond and the V−O bond orders of the three types of connectivity follow the order of V−O(-Te) < V−O(-V) < V−O(terminal).

Conclusion

In summary, a series of novel strontium(II) or barium(II) selenites and tellurites with additional V^{4+} or V^{5+} ions have been successfully prepared. They display six types of anionic structures, containing 0D $[(VO_2)(SeO_3)_2]^{3-}$ anion, three different 1D vanadium(V) tellurites chains, 2D $[(V_2O_5)_2(TeO_3)_2]^{4-}$ layer and 3D anionic framework of $[(VO)_3(SeO_3)_5]^{4-}$. The richness of the structure type of the vanadium tellurites or selenites can be attributed to the various coordination geometries of vanadium and various coordination modes for the tellurite and selenite anions. It is expected that many new vanadium tellurites and selenites with novel structures as well as new physical properties can be synthesized through hydrothermal reactions by changing the V/Te(Se) ratios.

Acknowledgment. This work was supported by National Natural Science Foundation of China (Nos. 20731006, 20825104, and 20821061) and the Knowledge Innovation Program of the Chinese Academy of Sciences.

Supporting Information Available: X-ray crystallographic files in CIF format, simulated and experimental XRD patterns, IR, optical diffuse reflectance spectra, band structures and total and partial densities of states (TDOS and PDOS). This material is available free of charge via the Internet at http://pubs.acs.org.

(27) (a) Godby, R. W.; Schluther, M.; Sham, L. *J. Phys. Rev. B* **1987**, *36*, 6497. (b) Okoye, C. M. I. *J. Phys.: Condens. Matter*. **2003**, *15*, 5945. (c) Terki, R.; Bertrand, G.; Aourag, H. *Microelectron. Eng*. **2005**, *81*, 514. (d) Jiang, H.-L.; Kong, F.; Mao, J.-G. *J. Solid State Chem*. **2007**, *180*, 1764.

(28) (a) Zhu, J.; Cheng, W.-D.; Wu, D.-S.; Zhang, H.; Gong, Y.-J.; Tong, H.-N. *J. Solid State Chem*. **2006**, *179*, 597. (b) Zhu, J.; Cheng, W.-D.; Wu, D.-S.; Zhang, H.; Gong, Y.-J.; Tong, H.-N.; Zhao, D. *Eur. J. Inorg. Chem*. **2007**, *2*, 285.